

Supplementary Information

Sulfide Sensor Based on the Room-Temperature Phosphorescence of ZnO/SiO₂ Nanocomposite

Na Wang^a, Ting Zhou^b, Jun Wang^a, Hongyan Yuan^{*a} and Dan Xiao^{*a, b}

^a*College of Chemical Engineering, Sichuan University, Chengdu 610065, P. R. China*

^b*Key laboratory of Green Chemistry and Technology, Ministry of Education, College of Chemistry,*

Sichuan University, Chengdu 610065, P. R. China

**Corresponding authors Tel: +86-028-85415029; Fax: +86-028-85416029*

E-mail address: yuan_hy@scu.edu.cn (Hongyan Yuan)

E-mail address: xiaodan@scu.edu.cn (Dan Xiao)

Table S1. The effect of the experiment conditions on phosphorescence intensity and spectra characteristics of the ZnO/SiO₂ nanocomposite and the sulfide detection ranges based on RTP of these materials.

Zn/Si (molar ratio)	Calcination temperature (°C)	Calcination time (h)	Phosphorescence intensity (a. u.)	Maximum excitation and emission wavelengths (nm)	Detection range (M)
1/99	500	2	116.2	320, 460	insensitive
5/95	500	2	582.2	320, 460	1.46×10^{-4} - 1.02×10^{-2}
8/92	500	2	719.36	320, 460	4.88×10^{-5} - 1.02×10^{-2}
10/90	500	2	781	320, 460	4.88×10^{-5} - 1.02×10^{-2}
12/88	500	2	577.68	320, 460	4.88×10^{-5} - 1.02×10^{-2}
15/85	500	2	642.92	320, 460	4.88×10^{-5} - 1.02×10^{-2}
20/80	500	2	641.96	320, 460	4.88×10^{-5} - 1.02×10^{-2}
10/90	400	4	140.64	280, 413	insensitive
10/90	450	3	552	280, 411	insensitive
10/90	550	1	736.32	280, 400	insensitive
10/90	550	2	1120.24	280, 380	insensitive
10/90	650	1	1511.28	280, 380	insensitive

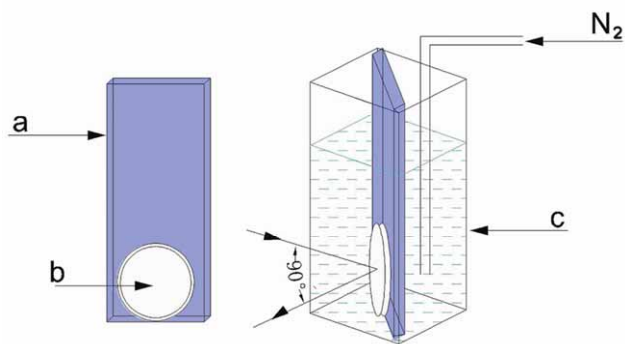


Figure S1. The diagram of the device for determination of Na_2S concentration. (a) glass slide (b) the disk of the ZnO/SiO₂ nanocomposite (c) quartz cuvette.

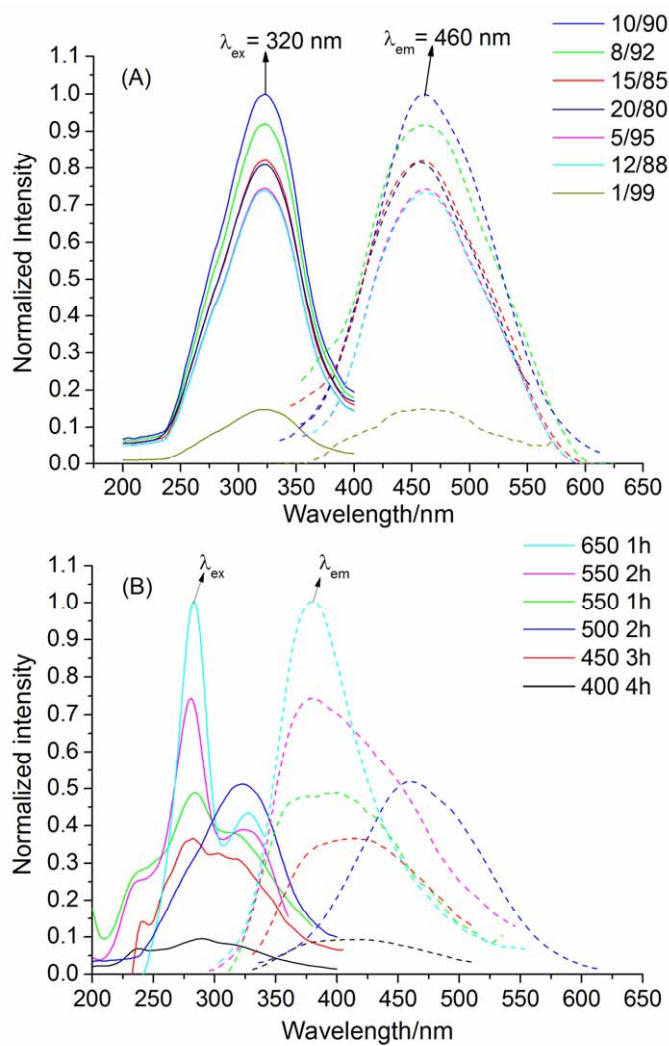


Figure S2. Excitation and emission phosphorescence spectra of ZnO/SiO₂ nanocomposite oxides obtained (A) with the different Zn/Si molar ratios under 500 °C for 2 h calcination and (B) under different calcination temperatures and time for the ZnO/SiO₂ nanocomposite with Zn/Si molar ratio = 10/90; solid lines are the excitation phosphorescence spectra and the dash lines are the emission phosphorescence spectra.

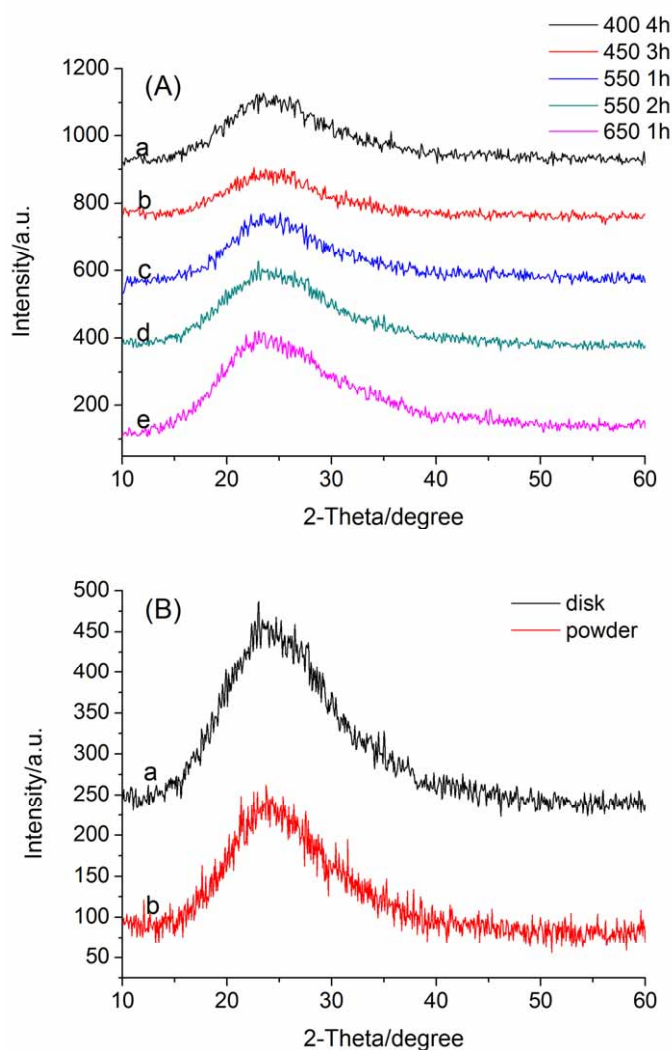


Figure S3. The XRD spectra of (A) the ZnO/SiO₂ with Zn/Si molar ratio = 10/90 obtained under different calcination conditions and (B) ZnO/SiO₂ with Zn/Si molar ratio = 10/90 obtained under 500 °C for 2 h of the (a) disk pressed used at 8 MPa and (b) powder.

It is clear from the results listed in the Table S1 and Figure S2 that the RTP emission mainly be divided into two processes: near ultraviolet (UV) emission and visible emission. Considering that neither the different calcination conditions nor the 8 MPa pressure to press the powder into a disk did not cause apparently phase changes in the materials (Figure S3), we ascribe the change of phosphorescence intensity and spectra to the competitive results of two radiative transitions (Figure S2 (B)). The UV

phosphorescence emission spectra of the material peaking at 380 nm is ascribed to the energy level of the donor state created by Zn-O-Si,²¹ which acts as traps for UV phosphorescence. And the visible phosphorescence spectra of the material peaking at 460 nm is ascribed to the surface defects of ZnO, *i.e.* oxygen vacancies, interstitial zinc and antisite defects on the surface of ZnO/SiO₂ nanocomposite (see Figure 5 and Figure 6). The number of phosphorescence traps varies with the calcinations temperature and time. The longer calcination time or higher calcination temperature perhaps increases the number of phosphorescence traps for UV emission and decreases that for visible emission.¹⁹ As a result, the increase of intensity for UV emission and the decrease of intensity for visible emission lead to a large blue shift of emission spectra.

Under the same calcination conditions, the phosphorescence intensity for ZnO/SiO₂ is shown to be a function of Zn/Si molar ratio. When the Zn/Si molar ratio increases from 1/99 to 10/90, the phosphorescence intensity of ZnO/SiO₂ increases rapidly with the increase of number of phosphorescence centers. When the concentration of Zn/Si molar ratio exceeds 10/90, the excessive Zn interferes with the phosphorescence centers resulting in the decrease of number of surface defects, *i.e.* self-quenching. Our previously work about the PbO/SiO₂ phosphor has the same self-quenching phenomena.⁸

8 T. Zhou, N. Wang, C. H. Li, H. Y. Yuan and D. Xiao, *Anal. Chem.*, 2010, **82**, 1705.

19 S. Chakrabarti, D. Ganguli and S Chaudhuri, *J. Phys. D: Appl. Phys.*, 2003, **36**, 146.

21 Z. P. Fu, B. F. Yang, L. Li, W. W. Dong, C. Jia and W. Wu, *J. Phys.: Condens. Matter*, 2003, **15**, 2867.

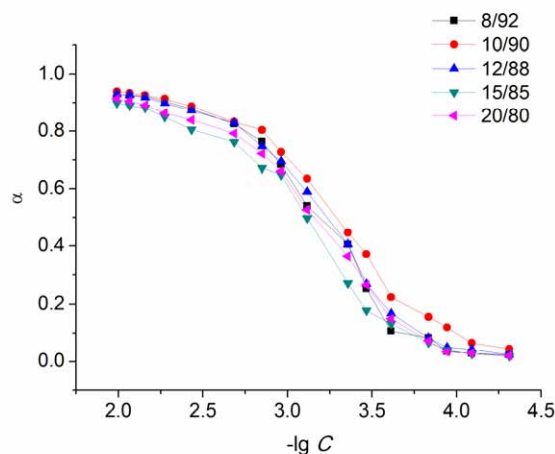


Figure S4. The response behavior of sulfide sensor. Plot of α versus $-\lg C$ of materials with different molar ratio of Zn/Si calcined at $500\text{ }^{\circ}\text{C}$ for 2 h ; $\alpha = (P_0 - P)/P_0$, P_0 and P are phosphorescence intensities of the sensor in the absence and in the presence of the sulfide, respectively, C is the concentration of sulfide.

All these materials were assayed for sulfide sensing as shown in Table S1 and Figure S4. The materials emitting UV emission band and that with a lower proportion of Zn are not sensitive to sulfide. Both the ZnO nanoparticles and SiO₂ matrix in the nanocomposite make the contributions to this UV emission band.²¹ However, sulfide reacts with ZnO to form ZnS while the SiO₂ matrix is almost not affected by the sulfide due to the chemical inertness of SiO₂ (see Figure 6). This may be the reason that the ZnO/SiO₂ nanocomposite emitting the UV phosphorescence is not sensitive to sulfide. On the other hand, the visible phosphorescence peaking at 460 nm originates from the surface defects of ZnO rather than the SiO₂ (see Figure 5 and Figure 6), thus this material is sensitive to sulfide without the contribution of SiO₂ to the visible phosphorescence emission. And for the materials with Zn/Si molar ratios of 1/99 and 5/95 calcined at $500\text{ }^{\circ}\text{C}$ for 2 h, the small number of binding sites could be responsible for their relatively insensitive response for sulfide sensing. The response behaviors of

sulfide sensor based on the ZnO/SiO₂ nanocomposites with the Zn/Si molar ratios ranging from 8/92 to 20/80 were tested to select the optimizing Zn/Si molar ratio. Their detection ranges are identical but their response behaviors are not. The response behavior of this sensor is dependent on the Zn/Si molar ratio of the material. When Zn/Si molar ratio increases from 8/92 to 10/90, the α value increases. As the phosphorescence emission spectra originate from the surface defects in ZnO, the material with a higher proportion of Zn has a larger number of surface defects resulting in the increase of the number of binding sites available for sulfide interaction. When the Zn/Si molar ratio increases from 10/90 to 20/80, the sensors have lower α values than that of 10/90. When Zn/Si molar ratio exceeds 10/90, the number of phosphorescence centers decreases caused by the self-quenching which reduces the number of binding sites available for sulfide interaction to quench the intensity of ZnO. The excessive nonphosphorescence Zn reacting to sulfide does not make contribution to sulfide sensing. As a result, the effect of self-quenching on the response behavior of sulfide detection causes that the materials of the Zn/Si molar ratios ranging from 12/88 to 20/80 for sulfide sensing are not as sensitive to sulfide ions as the material of the Zn/Si molar ratio = 10/90. It is concluded that the material of the Zn/Si molar ratio = 10/90 calcined at 500 °C for 2 h presents the best response to sulfide ions, which is used in the next experiments.

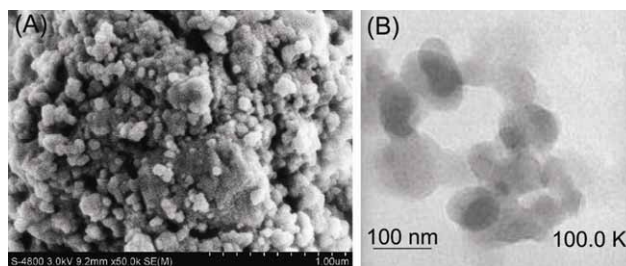


Figure S5. The (A) SEM and (B) TEM images of ZnO/SiO₂ nanocomposite.

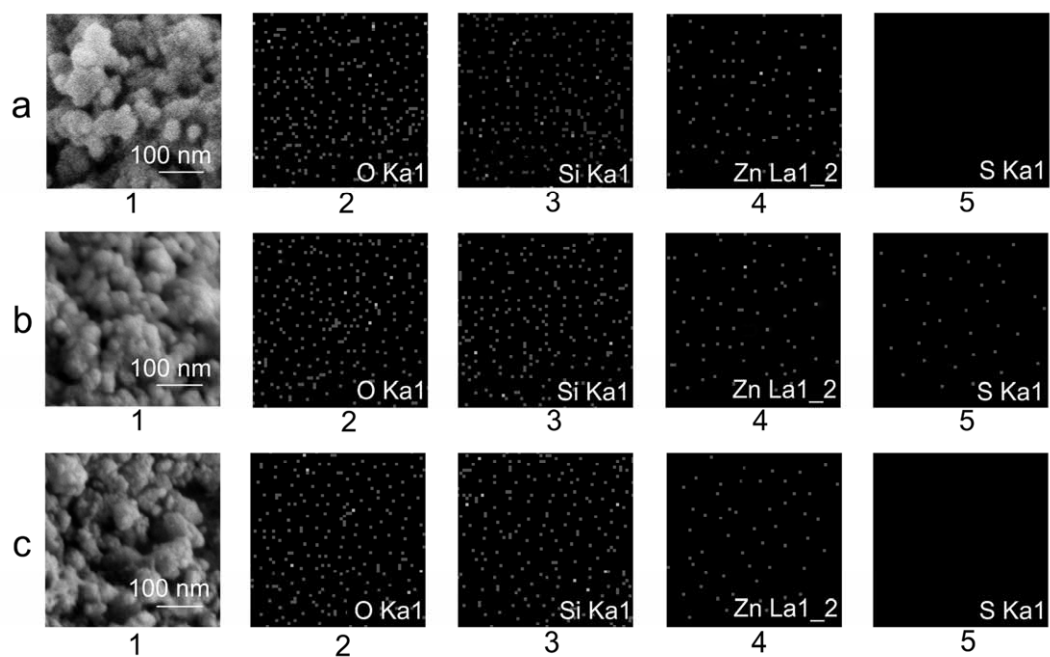


Figure S6. (1) SEM images and (2, 3, 4, 5) EDS images taken from the area of

ZnO/SiO₂ nanocomposite (a) before, (b) after interaction with Na₂S and (c) regenerated with H₂O₂.

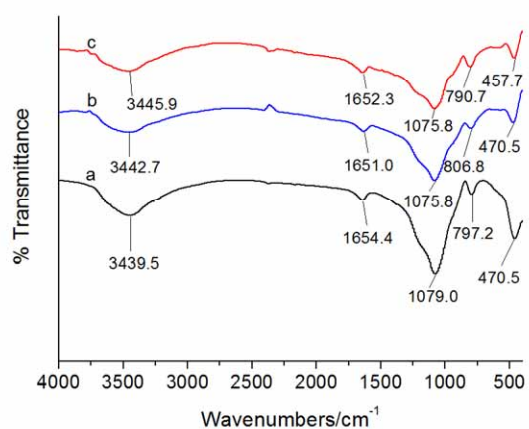


Figure S7. FT-IR spectra of (a) SiO₂ and the as-prepared ZnO/SiO₂ nanocomposite oxide (b) before and (c) after interaction with Na₂S.

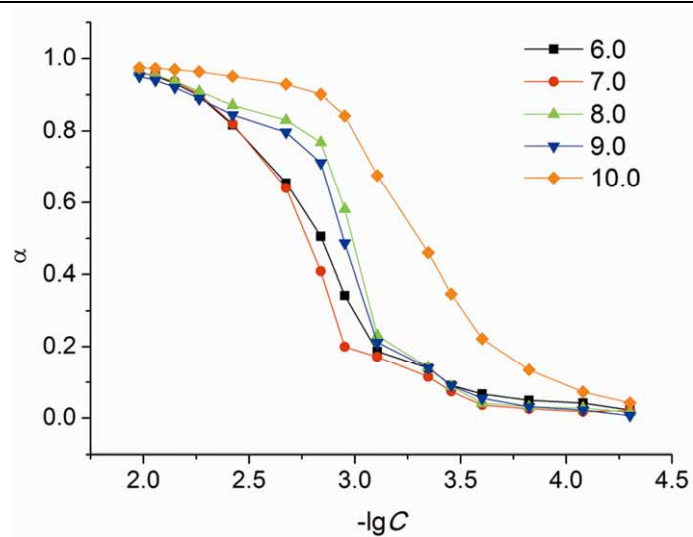


Figure S8. The response behavior of sulfide sensor. Plot of α versus $-\lg C$ at different pH values.

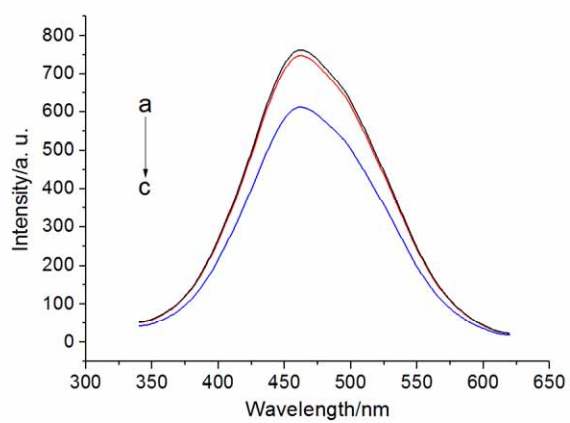


Figure S9. The phosphorescence spectra of ZnO/SiO₂ nanocomposite in different conditions: (a) original, regenerated (b) once and (c) twice by a H₂O₂ solution.

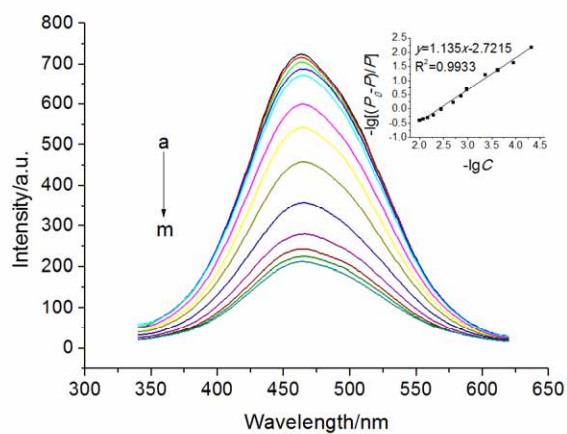


Figure S10. The effect of Na₂S concentration on the emission spectra of regenerated once sensor. The sulfide concentration: (a) 0, (b) 4.88×10^{-5} , (c) 1.14×10^{-4} , (d) 2.44×10^{-4} , (e) 4.39×10^{-4} , (f) 1.09×10^{-3} , (g) 1.42×10^{-3} , (h) 2.07×10^{-3} , (i) 3.69×10^{-3} , (j) 5.32×10^{-3} , (k) 6.95×10^{-3} , (l) 8.57×10^{-3} and (m) 1.02×10^{-2} M.

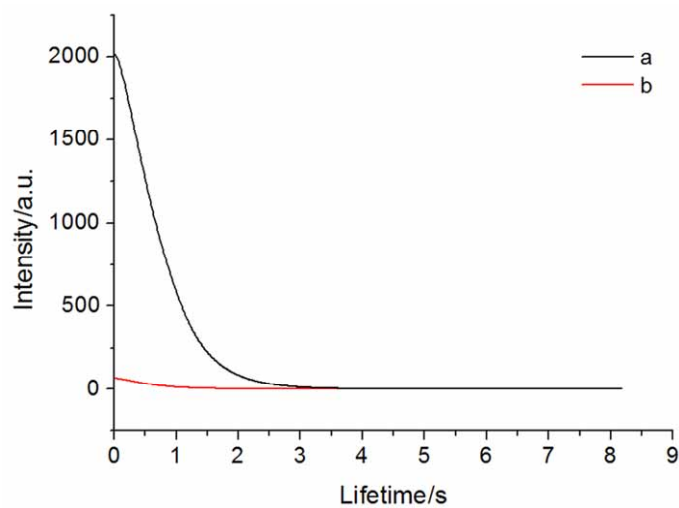


Figure S11. Decay of the phosphorescence intensity (a) ZnO/SiO₂ nanocomposite added PBS and (b) ZnO/SiO₂ nanocomposite added 0.01M Na₂S.

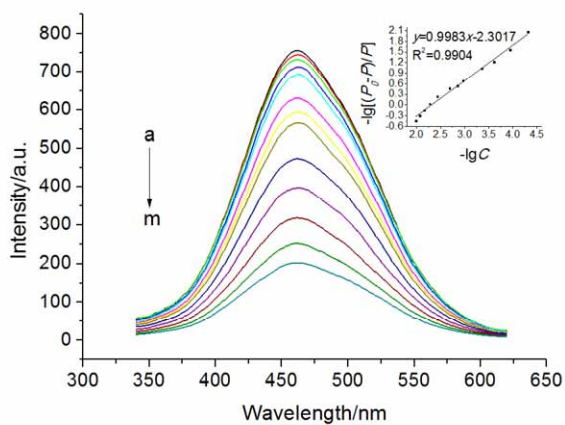


Figure S12. The effect of Na₂S concentration on the emission spectra of sensor stored for five and a half months. The sulfide concentration: (a) 0, (b) 4.88×10^{-5} , (c) 1.14×10^{-4} , (d) 2.44×10^{-4} , (e) 4.39×10^{-4} , (f) 1.09×10^{-3} , (g) 1.42×10^{-3} , (h) 2.07×10^{-3} , (i) 3.69×10^{-3} , (j) 5.32×10^{-3} , (k) 6.95×10^{-3} , (l) 8.57×10^{-3} and (m) 1.02×10^{-2} M.

UV lamp and RTP photographs

A hand-held UV lamp produces short and long wavelengths UV radiation at 254 nm and 365 nm, respectively. As shown in Figure 5A (b2) and (b3), after the phosphorescence intensity at emission wavelength of 460 nm being quenched by sulfide, the excitation and emission wavelength change to 350 nm and 490 nm, respectively. As a result, when employing the UV radiation at 365 nm as the excitation light source, there are nearly no differences in the RTP intensity of the sensor with the addition of different concentrations of Na₂S. We could only chose the UV radiation at 254 nm as the excitation light source to take the RTP photographs. And in view of the excitation wavelength of the ZnO/SiO₂ nanocomposite at 320 nm, the phosphorescence intensity upon excitation at 254 nm was nearly completely quenched by 1.00×10^{-2} M Na₂S as shown in Figure 4B (d).